Prediction of percentage of ferrite as a function of heat input in robotic gas metal arc welding of duplex stainless steel SAF 2205 Welds

Payares-Asprino, Maria Carolina; Muñoz-Escalona, Patricia

Published in:
Proceedings of ESSC & DUPLEX 2019

Publication date:
2019

Document Version
Author accepted manuscript

María Carolina Payares-Asprino[1], Patricia Muñoz-Escalona[2]

[1]Norwich University, Mechanical Engineering Dept. 158 Harmon Drive, Northfield, Vermont 05663, USA

[2]Glasgow Caledonian University, School of Computing, Engineering and Built Environment Glasgow, G4 0BA, UK.

PREDICTION OF PERCENTAGE OF FERRITE AS A FUNCTION OF HEAT INPUT IN ROBOTIC GAS METAL ARC WELDING OF DUPLEX STAINLESS STEEL SAF 2205 WELDS

María Carolina Payares-Asprino[1], Patricia Muñoz-Escalona[2]

[1]Norwich University, Mechanical Engineering Dept., 158 Harmon Drive, Northfield, Vermont 05663, USA

[2]Glasgow Caledonian University, School of Computing, Engineering and Built Environment Glasgow, G4 0BA, UK.

Abstract

Dual phase duplex stainless steels with ferrite and austenite as part of their microstructure have shown an outstanding strength and corrosion resistance despite of the aggressive and hostile environments they can be subjected to. In the last years a worldwide rapid growth demand and consumption of duplex stainless steel, particularly in petrochemical, marine, power plant, food industry and other engineering applications have taken place especially where welding processes were required. Joining of duplex alloys is a challenging task, due to the formation of embrittling precipitates and metallurgical changes they go through during the welding process. Generally, the quality of a weld joint is strongly influenced by the welding conditions and imbalance phase ratio between the austenite and ferrite, these factors leads to solidification cracking, corrosion susceptibility, and lower ductility. To achieve high quality welds mathematical models have been developed in order to predict the ideal bead geometry to achieve optimal mechanical properties. This paper focuses on determining the percentage of ferrite in GMAW welds of duplex stainless steel SAF 2205. An experimental model for the prediction of weld bead geometry was developed and applied. The values of weld penetration and reinforcement areas were calculated using a statistical approach and the amount of ferrite in the duplex stainless steel welds were determined applying the rule of mixture and the Schaeffler diagram. These predicted values of ferrite were later on compared with experimental values obtained through chemical. The results indicate 0.7% of error between experimental and predicted values of ferrite when using heat inputs higher than 0.9kJ/mm

Keyboards

Robotic GMAW welding, Weld penetration, Weld reinforcement, Duplex stainless steels, Rule of Mixture, Ferrite Content.

1. Introduction

Duplex stainless steels (DSS) are widely used in many engineering applications such as those found in the petrochemical, pulp and paper, and oil and gas industries, since they exhibit good mechanical properties and high corrosion resistance. Properties such as high tensile strength, high fatigue strength, good toughness even at low temperature, adequate formability and weldability and excellent corrosion resistance (e.g. stress corrosion cracking and pitting) result from the almost equal amount of ferrite (α) phase and austenite (γ) phase present in this steel. The presences of these two phases combine the attractive properties of austenitic and ferritic steels [1-4]. There is an increase used of DSS in the pipe industry compared to austenitic stainless steels, particularly where chloride or sulphide stress corrosion cracking is of primary concern [5]. However, the solidification of duplex stainless steel welds does not always produce near equal amounts of ferritic (α) and austenitic (γ) phases, as occurs in the parent metal; thus deteriorating the mechanical properties and corrosion resistance of the weld joint. The microstructures developed in the weld's fusion zone and the heat-affected zone (HAZ) also have a significant influence on the mechanical properties and corrosion resistance of duplex stainless steels [3-6]. To guarantee the excellent combination of properties in DSS, it is essential to maintain a ferrite-austenite ratio close to 50:50. This phase balance however changes during the welding process due to the rapid cooling process involved in most thermal cycles, resulting in weld ferrite contents with an excess of 50%. In order to restore the phase balance, weld filler materials usually alloyed with 2-4% more of Ni compared to the base metal are used [7,8]. Hsieh et al. [9] reported that the austenite contents lower than 25% are unacceptable for most industrial application, since excessive ferrite in the heat-affected zone (HAZ) and weld metal (WM) causes a loss of toughness and a decrease in corrosion resistance. Norsok standard recommended that a minimum in austenite content of 30% is required to accept the welded pipes [10].

Various researchers reported that controlled heat input is the most important factor in order to maintain the phase balance after the welding process of DSS. Other researchers [11-13] reported that the cooling rate is the parameter that controls the phase balance in weldments, and also dictates the heat input range to be used. Giridharan et al. [14] reported that heat input has a significant impact on the bead geometry, metallurgical, mechanical and corrosion resistance properties of the welds. Similarly, Karunakaran [15] reported that the rate of heat input during welding followed by the nature of cooling has a strong influence on the grain's size and phase formation. Recommendations in relation to super-duplex stainless steels have also been made, where a moderate heat input should be used (depending on material's thickness and joint's geometry) in order to obtain beneficial outcomes such as corrosion resistance [16]. From the open literature it is well inferred that a low heat input and a fast cooling rate produces the formation of Cr_2N precipitation and higher heat inputs lead to the formation of X or σ phases which have been reported as deleterious phases affecting the mechanical properties of weldments [17, 18]. Hence, the importance of using an optimal heat input to control the formation these phases. With regards the arc current Ozlati et.al reported that the strength resistance of welds conducted on duplex stainless steel rod decrease with when increasing arc current [19]. Other researchers formulated empirical models that are able to predict the approximate weld bead contour of duplex stainless steel welds from established ranges of welding parameters [20,21].

This present work focuses on the influence of heat input on the percentage of ferrite in duplex stainless steel welds. The cross-sectional area of weld reinforcement and weld

penetration were calculated using a developed mathematical model and these values were used to predict the percentage of ferrite using the Rule of Mixture and Schaeffler Diagram [22].

2. Experimental Procedure

2.1 Workpiece Characteristics

Duplex Stainless Steel SAF 2205 was selected as parent material as it is widely used in the petrochemical industry. Table 1 shows the chemical composition of SAF 2205 DSS and filler metal ER-2209 (electrode) of 1 mm diameter as recommended by ASTM A815 and A789 procedures GMA welding process.

Table 1. Chemical composition of the DSS SAF 2205 plate and ER 2209 filler metal

Material	%C	%Si	%Mn	%P	%S	Cr	Ni	Mo	N
SAF 2205	0.045	0.32	1.41	0.030	0.020	22.32	5.31	3.34	0.08
ER 2209	0.015	0.54	1.87	0.023	0.006	23.31	9.81	3.77	0.14

2.2 Welding Parameters.

Single bead-on-plate welds were developed using GMA welding (*FANUC 100iB®*) on DSS under different welding conditions. Equation 1 was used for heat input calculations, where recommended values for heat input ranged between 0.5 and 2.5 kJ/mm for stainless steel duplex SAF 2205 [2]. The bead-on-plate (BOP) welds were manufactured using the conditions shown in Table 2. Figure 1 shows a Schematic drawing of the Bead on Plate (BOP) welds and dimensions of the plate.

$$HI\ (Heat\ input) = \frac{Arc\ current\ x\ Arc\ voltage\ x\ 60}{Welding\ speed\ x\ 1000} \qquad (1)$$

Where

$$HI\ (\mathrm{kJ/mm}), Arc\ Voltage\ (\mathrm{V}), Arc\ Current\ (\mathrm{A}), Welding\ speed\ (\mathrm{mm/min}).$$

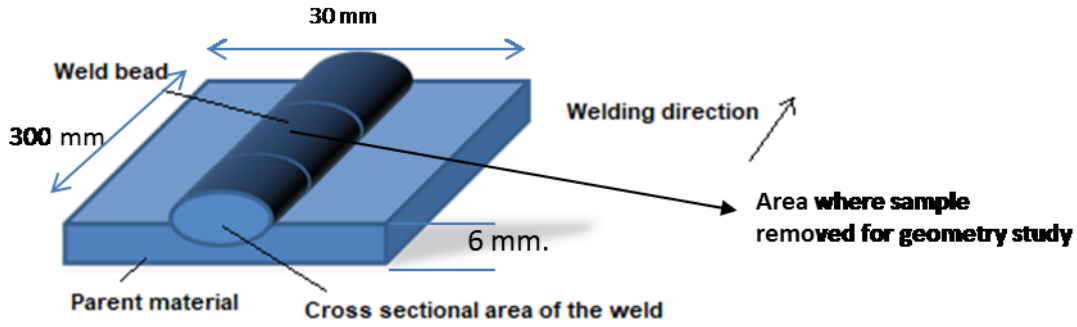

Fig.1. Schematic drawing of the Bead on Plate (BOP) welds

As it is known, robots (automatic welding) only allow to set the arc voltage, the wire feed transfer (WFT) and the welding speed during the welding process. In order to obtain values of arc current, a graph of arc current vs WFT was developed based on data collected from the robot. The developed graph and a mathematical expression of arc current as a function of WFT is shown in Figure 2.

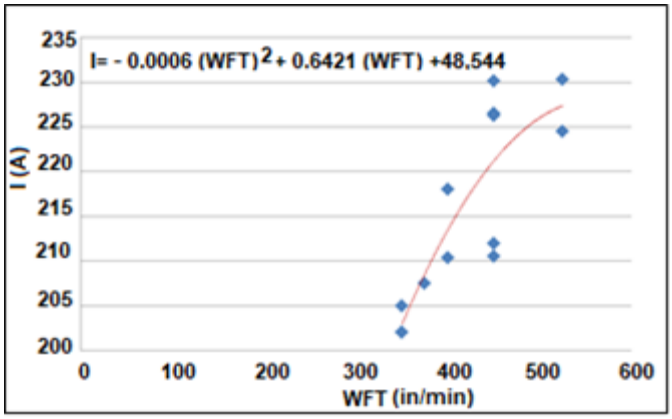

Fig. 2. Arc current vs WFT for FANUC 100iB

To study the weld bead cross sectional area geometry, a small sample was cut from the weld track 150 mm away from the weld's starting point (middle of the weld track) where welding parameters are stabilized (see Fig 1). Table 2 shows the combination of welding variables used and resulted heat input. All samples, 13 in total were metallographic prepared following ASTM E3-01 standard and then etched with Kalling # 2 (5g de $CuCl_2$, 100ml Ethanol, 100ml HCl and 100 ml H_2O).

Table 2. Selected welding parameters

Sample	Arc Voltage (V)	WFT (in/min)	Arc Current (A)	Welding speed (mm/min)	Heat Input (kJ/mm)
1	28.00	450.00	212.00	480.00	0.740
2	28.00	525.00	224.50	480.00	0.790
3	28.00	450.00	210.50	300.00	1.180
4	28.00	525.00	230.30	300.00	1.290
5	28.00	525.00	230.30	300.00	1.900
6	30.00	350.00	202.00	480.00	0.760
7	30.00	450.00	230.13	480.00	0.860
8	30.00	350.00	205.00	300.00	1.230
9	30.00	450.00	235.00	300.00	1.410
10	30.00	375.00	207.50	300.00	1.250
11	30.00	450.00	226.25	300.00	1.360
12	30.00	350.00	202.00	360.00	1.010
13	30.00	400.00	218.00	300.00	1.310

The chemical composition of each sample was obtained conducting a spectrographic chemical analysis SPECTROLAB 5L and following ASTM A1016 standards. Since chemical composition were similar for similar values of heat input, these were re-arranged in 3 groups for simplicity purposes These values are reported in Table 3

Table 3. Results of the spectrographic chemical analysis for different heat inputs.

HI (kJ/mm)	%C	%Si	%Mn	%Cr	%Mo	%Ni	%Nb
0.8	0.0490	0.399	1.7110	21.7900	3.4970	7.0400	0.0059
1.0	0.0398	0.4411	1.6870	21.8800	3.5630	7.5300	0.0077
1.4	0.0433	0.4177	1.7250	21.9300	3.4270	7.3000	0.0153

3. TECHNICAL APPROACH

3.1. Estimation of %Ferrite through rule of mixture

3.1.1. Rule of Mixture (Predicted values)

The percentage of ferrite content in the weld's fusion zone generated through a GMAW process was obtained using the rule of mixture shown in Equation 2 [24].

$$\left[\%X_{weld}\right] = \frac{B}{B+D} \cdot \left[\%X_{BM}\right] + \frac{D}{B+D} \cdot \left[\%X_{FW}\right] \qquad (2)$$

where:

$\%X_{weld}$ is element percentage content in the fusion zone.
$\%X_{BM}$ is element percentage content in the base metal.
$\%X_{FW}$ is element percentage content in the filler metal.
B is the area of penetration of the weld.
D is the reinforcement area.

i) Dilution for GMAW Welds

Weld dilution was determined using metallographic methods by measuring the individual cross-sectional areas of the deposited filler metal and melted substrate. The ratio of the melted substrate (B) to the total melted cross-sectional area from the filler metal and substrate ($B+D$) describes the level of dilution:

$$Dilution = \frac{B}{B+D} \qquad (3)$$

Note that the area of the melted substrate (on a transverse cross-section) B represents the penetration area of the weld, and D represents the reinforcement area of the weld.

ii) Calculation of experimental weld bead's cross sectional area geometry contour

In order to predict the %Ferrite using the rule of mixture equation, calculations of the experimental weld's cross sectional area geometry contour is required. For this purpose photographs of the samples cut from the welded track were obtained using an optical microscope Olympus BX53M. Each image was uploaded in Mathematica 7 ® software for processing.

More than one hundred (100) points were used to develop the contour of the cross sectional area geometry of the weld bead. This allowed to produce a representation in Cartesian coordinates (X-Y) for each combination of welding parameters (13 samples-Table 2). Once the cross sectional area geometry contour was completed, the Mathematica 7 ®

Software allowed for the calculation of the centroid of the generated shape based on the geometry developed through the combination of the welding parameters [23].

3.2. Estimation of %Ferrite through Shaeffler's Diagram (experimental values)

To estimate the % ferrite thought the Schaeffler's diagram, it is necessary to calculate the nickel and chromium equivalent using Equations 4 and 5 respectively [22]. These values of Ni_{eq} and Cr_{eq} were obtained by substituting the values of chemical analysis obtained through the spectrographic chemical analysis and reported in Table 3. The results were later plotted on the Schaeffler diagram to predict % ferrite as indicated in Figure 3.

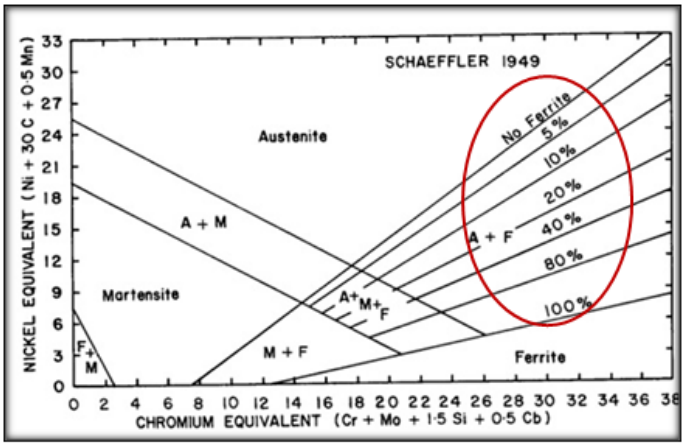

$$Ni_{eq}=\%Ni+30\%C+0.5\%Mn \quad (4)$$

$$Cr_{eq}= \%Cr+\%Mo+1.5\%Si+0.5\%Nb \quad (5)$$

Fig 3. Shaeffler Diagram [22]

4. Results and Discussion

4.1 Prediction of reinforcement area and penetration area of weld bead using the Experimental Model for GMAW welds.

Figure 4a show an example of photographs of the cross sectional geometry of the weld bead on DSS weld and Figure 4b its digital contour representation of the cross sectional area's geometry. The centroid of the developed contour was obtained through electron microscope using a JEOL JSM -5800.

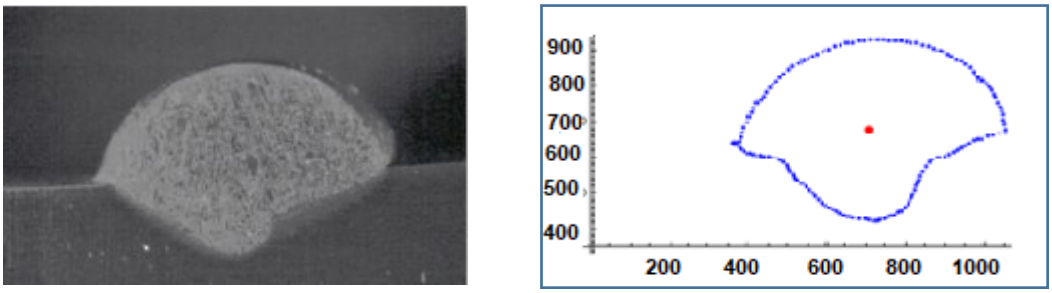

a) b)

Fig.4. Cross sectional area of weld bead when using 224.5A, 28V and 480 mm/min taken 150 mm away from weld's starting point. a) Image of cross sectional area and b) Digital representation obtained through Mathematica 7. The centroid of the developed contour is indicated with red dot

Once the digital contour for each 13 condition was developed, the image was rotated and translated to Cartesian axes as shown in Figure 5.

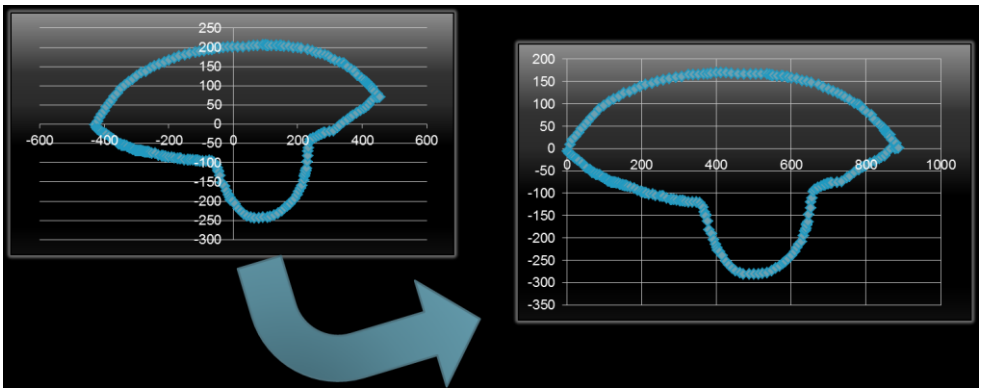

Fig. 5. Rotation and translation the developed contour in Cartesian axes for a weld developed using 230.13A, 30V and 480 mm/min

It must be highlighted that X and Y axis represent number of pixels which were later transform in a program that was set-up to run on windows, where welding parameters were used as input values and the outputs are the cross sectional area's geometry and contour as observed in Figure 6, where values of height of the reinforced area and value of depth of penetration as well as the width of the weld are calculated based on numbers of pixels obtained in the geometry's contour.

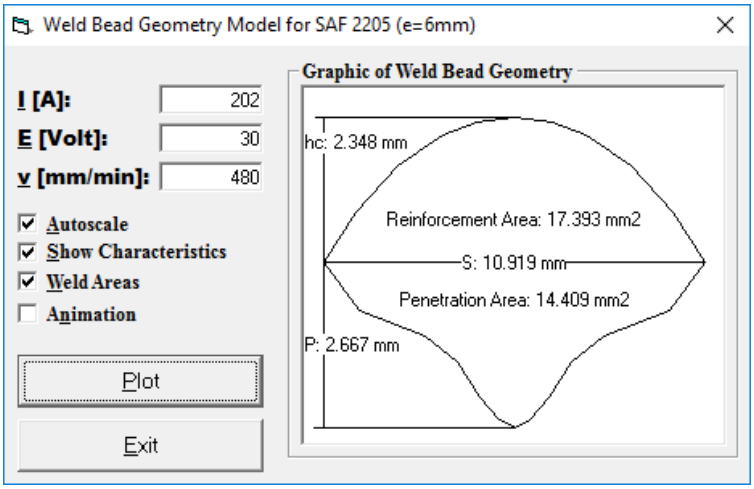

Fig. 6. Example of the contour of the weld bead geometry

4.2 Comparison of % predicted and experimental values of %Ferrite Content of DSS Welds

Experimental and predicted values of %Ferrite obtained through Schaeffler diagram and rule of mixture respectively are shown in Figure 7 for different values of heat inputs.

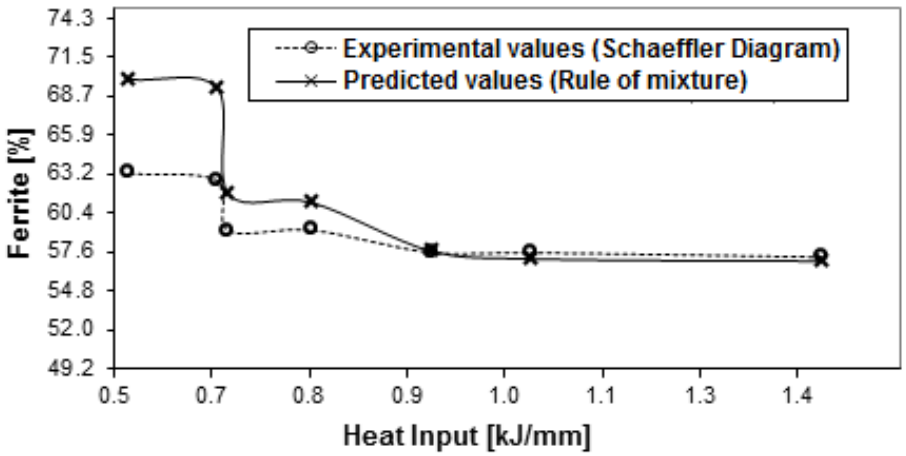

Fig. 7. Comparison of predicted and experimental values of %Ferrite vs Heat input

When analysing Figure 7, it is observed how %Ferrite decreases when increasing the heat input. The results are very encouraging especially for HI >0.9 kJ/mm where the predicted and experimental values are very similar, with an error of 0.7%. For HI< 0.9 kJ/mm a maximum error of 10% between predicted and experimental values was obtained when using HI values near 0.5 kJ/mm. This result is in agreement with Mohammed et.al who reported that low heat input results in high volume of fractions of ferrite [25].

5. Conclusions:

- The developed model is capable of predicting geometry of the weld's reinforcement and penetration of DSS welds
- The developed model showed to provide reliable results when using it for the estimation of %Ferrite content through the rule of mixture.

- The ferrite content in the fusion zone decreased with increasing heat input for DSS ROBOTIC GMAW welds for all the methods studied.
- Welds manufactured using similar heat inputs resulted in similar chemical composition content

6. References:

[1] *AVESTA WELDING.* How to Weld AVESTA SHEFFIELD 2205 *Sweden. Trade Literature.*
[2] AK Steel, "Duplex Stainless Steels SAF 2205", USA. 2004.
[3] N.G. Robert , Duplex Stainless Steels Microstructure, Properties and Applications, Abington Publishing, Cambridge, 1997. 2841-2856.
[4] T.H. Chen. J.R. Yang, Microstructural characterization of simulated heat affected zone in a nitrogen-containing 2205 duplex stainless steel Mater. Sci. Eng. A (2002, Volume 338) p 166.
[5] H.Y. Liou, R.I. Hsieh, W.T. Tsai, Microstructure and stress corrosion cracking in simulated heat-affected zones of duplex stainless steels, Corro. Sci. (2002, Volume 44) p.2841.
[6] M.A. Miranda, J.M. Sasaki, S.S.Tavares, The use of X-ray diffraction, microscopy, and magnetic measurements for analysing microstructural features of a duplex stainless steel Mater. Character, (2005, Volume 54) p. 387.
[7] M. Liljas, Proceeding of the Fourth International Conference of Duplex Stainless Steels, Glasgow Scotland, paper 7, Vol. 2, pp113-16, November 1994.
[8] N. Stephenson, Welding status of duplex stainless steels for offshore application–Part I. and Metal Fabrication, (1981,Volume 5) p 159.
[9] R.I. Hsieh, HY Liou, Y.T. Pan., Effects of cooling time and alloying elements on the microstructure of the gleeble-simulated heat-affected zone of 22% Cr duplex stainless steels, J. Mater. Sci. Perfor. (Volume 10), p.526.
[10] Norsok StandardM601-94. Welding and Inspection Piping. Lysaker Norway: Standard Norway; 2004.
[11] C.F.G, Baxter, J. Irwin, R. Francis. Proceeding of Intern. Offshore and Polar Eng. Conf. Conf. on Duplex Stainless Steel on Glasgow, (1993,Volume 2) p. 401.
[12] M. Liljas . Proc. Of the Fouth Intern. Scotland, Keynote(1994, Paper V) p.13.
[13] JC, Lippold, D.J Kotecki. Welding Metallurgy and Weldability of Stainless Steel . New York: Willer Inder Science Publication; 2005.
[14] P.K. Giridharan, N. Murugan N. Optimization of pulsed GTA welding process parameters for the welding of AISI 304L stainless steel sheets Int. Adv. Manuf. Technol. (2009, Volume 2) p. 478.
[15[N.Karunakaran, V.Balasubramanian, Effect of pulsed current on temperature distribution, weld bead profiles and characteristic of gas tungsten arc welded alloy joints Transactions of Nonferrous Metals Society China, (2011, Vol. 21, Issue 2) p. 278.
[16] ASM Speciality Handbook on Stanless Steels. American Society for Metals; Ohio,1994.
[17] V. Muthupandi, P. Bala Srinivasan, SK. Seskadri, Effect of weld metal chemistry and heat input on the structure and properties of duplex stainless steel welds, Mat. Sci. Engineering A (2003 Vol. 358, p. 9)
[18] M Yousefieh, M. Shamanian, A. Saatchi, Influence of Heat Input in Pulsed Current GTAW Process on Microstructure and Corrosion Resistance of Duplex Stainless Steel Welds, Journal Iron Steel Rese Int. (2011,Volume 18(9)) p.65
[19] Ozlati, M. Movahedi. Journla of Manuf. Processses Vol. 35, pp. 517-525, 2018
[20] M.C. Payares and M. Dorta Almenara, Mathematical Expression for the Prediction in

Butt Joints for Duplex Stainless Steel SAF, ASME International Mechanical Engineering Congress and R&D Expo, Washington, D.C., (2003).
[21] V. Dey, D. Kumar Pratihar, G.L. Datta, M.N. Jha, T.K. Saha, A.V. Bapat, Optimization of bead Geometry in electron Beam welding using a Genetic Algorithm, Journal of Mat. Processing Tech. (2009, Volume 209) p.1151.
[21] I.S.Kim, J.S. Son, C.E. Park, C.W. Lee, Yarlaggadda K.D.V. Prasad, A study on Prediction of Bead height in Robotic arc Welding using neural network.
[22] A. Schaeffler, A Diagram is given for Estimating Microstructures of Weld Deposits in Types 308, 309, 309 Cb, 310, 312, 316, 317, and 318 Stainless Steels, Metal Progress, (1949, Volume 56, N.11) p.680.
[23] Steele J., Payares, C. Mathematical Modeling of Weld Bead Profile Shapes: Modeling and Measurements. *88th AWS Annual Convention*, Las Vegas, 2008.
[24]GRONG, Ø, Metallurgical of Welding. The Institute of Materials, England, 1997, pp.1-12.
[25] G.R.Mohammed, I.Mahazdzir, S.N. Aqida, H.A. Abdulhadi, Effects of Heat Input on Microstructure, Corrosion and Mechanical Characteristic of Welded Austenitic and Duplex Stainless Steel: A Review, Metals, (2017, Vol.17) p.39